Indian Journal of Chemical Technology
Vol. 27, May 2020, pp. 227-234

A simple strategy to increase inhibitory activity of chitosan towards iron corrosion in acidic media

Zahra Yavari*[,1,2], Salameh Nematiyan[1], Hamideh Saraveni[1] & Meissam Noroozifar*[,1,2,3]

[1]Department of Chemistry, University of Sistan and Baluchestan, Zahedan, P.O. Box 98135-674, Iran

[2]Renewable Energies Research Institute, University of Sistan and Baluchestan, Zahedan, Iran

[3]Department of Physical and Environmental Sciences, University of Toronto Scarborough 1065 Military Trail, Toronto, Ontario, M1C 1A4, Canada

E-mail: z_yavari@chem.usb.ac.ir, m.noroozifar@utoronto.ca

Received 18 September 2019; accepted 8 April 2020

The chitosan as a natural and inexpensive polymer is considered as an appropriate choice towards the corrosion inhibitory. Here, the corrosion and inhibition efficacy of iron sheets is examined in the H_2SO_4 solution and the presence of chitosan and potassium iodide as an inhibitor through gravimetry, potentiodynamic polarization, and impedance analyses. The inhibition performance is found to be enhanced by adding chitosan concentration. The experimental data demonstrate that the doping iodide ion to chitosan is efficient on the surface coverage and the inhibition performance. The introduced inhibitors are of the interface inhibitors → liquid phase → mixed type with the physical adsorption. The adsorption of iodized chitosan on the iron surface is followed Langmuir isotherm. These inhibitors, by changing the electrical double layer, increase the resistance of charge transfer. The existence of iodide in the chitosan structure improves the electron density of polymer and strengthens the interaction between inhibitor and metal.

Keywords: Chitosan, Corrosion inhibitor, Potassium iodide, Iron, Surface coverage

The acids are among the most widely used electrolytes in different industrial processes. They are employed in chemical cleaning and industrial pickling processes. On the other, iron is one of the most essential metals in the industry. So, the ferrous components can be significantly used in many industrial constructions including the fluid transfer pipes and the power plants. Therefore, the iron corrosion in acidic medium poses major economic problems for industries included reducing the thickness of the metal structure when the corrosion product be soluble like Fe^{+2} [Ref.1]. Appropriate approaches can be utilized to decrease the iron corrosion, and one of them is the employing chemical components as inhibitors[2]. They are adsorbed on the iron surface, so obstructing the iron from coming into interaction with the corrosive agents[3]. The inhibitor features included molecular volume, molecular mass, and parameters of geometric and electronic are affecting on the inhibitor adsorption onto the surface of metal[4]. The existence of heteroatoms (e.g., N and O) and double bonds in the compound structure affects the electron density of the inhibitor as an electronic parameter[5]. An interaction occurs between the inhibitor with high electron density as a donor and the metal with the vacant or partially filled d orbital as acceptor; so a proportional bond would be created[6].

In recent years, polymers have been considered as useful inhibitors for the corrosion reaction of different metals[7,8]. Deacetylchitin known as chitosan [2-amino-2-deoxy-(1-4)-β-D-glucopyranose] is a water-soluble cationic hetero-polymer which is fabricated by de-acetylation of chitin, a chemical structure with acetyl-glucosamine units (Fig. 1)[9]. Chitosan can be an appropriate option for use in industrial applications due to its biocompatibility, biodegradability, nontoxicity, and adsorption attributes[10]. The halides presence in the polymer structure as inhibitor has already been considered by Larabi *et al.*[11] and Chetouani *et al.*[12].

The present paper describes improving the inhibitory activity of chitosan in iodine presence for corrosion of iron in acidic electrolyte. Four samples of chitosan-iodide were prepared with different ratios as the inhibitor of corrosion for iron in sulfuric acid medium. The inhibition performance of samples was evaluated via the corrosion tests such as weight-loss test or gravimetric analysis, Tafel linear polarization,

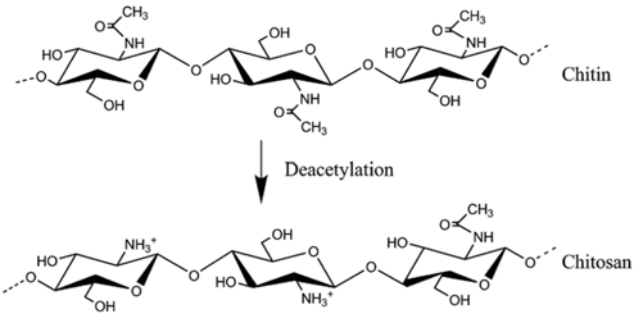

Fig. 1 — Structure of chitin and chitosan [9].

and impedance electrochemical spectroscopy. Also, the morphology of the iron surface was studied via the scanning electron microscope in the absence and presence of the inhibitors.

Experimental Section

Chemicals

Chitosan with 400,000 Da molecular weight was supplied from Fluka. Other reagents were provided from Merck Company. Bidistilled water was used to prepare test solutions. The materials were used without additional purification

Instrumentation

An analytical balance CP224S model manufactured by Sartorius, Germany, were used to weighing the materials with an accuracy of 0.0001 g. A three-electrode SAMA 500 electro-analyzer constructed by Isfahan, Iran Research Center was utilized to investigate linear polarization and open circuit potential (OCP). An auto-lab PGSTAT 128N (EcoChemie, Netherlands) potentiostat/galvanostat directed by NOVA 1.11 carried out electrochemical impedance spectroscopy (EIS) examination. The surface morphology of iron specimens was observed with a scanning electron microscope (SEM, KYKY EM3900). A ball mill laboratory (Shimadzu Ball Mill 25796) was used to reduce the particles size.

Synthesis of inhibitors

The inhibitors samples were obtained by mixing chitosan and potassium iodide in 0.5 M hydrochloric acid for 4 h with different weight ratios of chitosan to KI such as 4:0, 3:1, 2:2, and 1:3 were denoted as CH, CH-I, CH-2I, and CH-3I, respectively. At the end of the mixing time, the resulting sediments were filtered by a Buchner funnel and the Whatman filter paper of grade 1 and washed with the bidistilled water. The precipitates were dried at 50°C for 12 h. Finally, the sediments were powdered using a ball mill.

Preparation of iron specimens

For gravimetric and microscopic studies, the iron sheets with 1 mm thickness were cut in 1 × 1 cm^2 dimensions and the specimens edges were straightened with a rasp. Also, the iron cylinder, fixed in epoxy coating with a bare area of 1.0 cm^2 to the electrolyte, served in electrochemical studies. Before all tests, the specimens were polished by using SiC papers from 600 to 1000 grade to create a mirror-like surface, washed with acetone and deionized water; then dried at room conditions.

Weight loss test

The weighed iron specimens were immersed at an inclined position in 50 mL solution of 0.5 M sulfuric acid and a specific concentration of inhibitor (0, 0.1, 0.3, and 0.5 g/L) at 30, 40, 50, and 60°C for 2 h. At the ending immersion, the specimens were withdrawn, washed with the distilled water, and acetone, dried and weighed. Finally, weight loss (W) was calculated.

Scanning electron microscopy

The iron specimens were immersed in an aqueous 0.5 M sulfuric acid containing 5 g/L inhibitor. Also, an iron specimen as blank was placed in the acid solution without any inhibitor. After 5 h, the specimens were withdrawn, washed with the distilled water, and acetone, dried and sent for microscopic studies in zipped plastic bags under nitrogen gas.

Electrochemical studies

The iron specimen (prepared according to 2.4. section) was served as a working electrode. A Pt electrode was employed as a control electrode. The references electrode was a saturated calomel electrode (SCE) and Ag/AgCl for polarization and EIS studies, respectively. The electrolyte was the de-aerated 0.5 M H_2SO_4. At first, the OCP was recorded for 1000 s, and the potential range was selected as $E_{OCP} \pm 0.25$ V. The potentio-kinetic current and voltage characteristics were collected with a scan rate of 0.01 Vs^{-1}.

Results and Discussion

Weight loss analysis

The iron dissolution in an acid and the relevant reactions are as follows[13]:

$$Fe \rightarrow Fe^{2+} + 2e^{-} \quad \ldots (1)$$

$$2H^{+} + 2e^{-} \rightarrow 2\,H_{ads} \rightarrow H_2 \quad \ldots (2)$$

The high products solubility after iron corrosion leads to a weight loss of metal in acidic solution. Based on gravimetric tests, the corrosion rate (CR) in $gcm^{-2}h^{-1}$ was calculated by[14]:

$$CR = \frac{W}{A \times t} \quad \ldots (3)$$

A and t are the exposed area and the immersion time, respectively. The inhibition efficiency (%IE) is obtained by [15]:

$$IE\% = \frac{W_0 - W}{W_0} \times 100 \quad \ldots (4)$$

where W_0 and W be the weight loss of iron specimens in the absence and presence of inhibitor, respectively. The surface coverage (θ) was represented as[16]:

$$\theta = \frac{IE\%}{100} \quad \ldots (5)$$

Table 1 displayed the results and computation relative to weight loss test for iron specimens without and with inhibitor at 30°C and for 2 h. According to Table 1, in the presence of the inhibitor, the amount of weight loss and corrosion rate were dropped to the inhibitor absence. It proves that these polymeric components have inhibitory properties. The corrosion rate was reduced to rise the inhibitor concentration; while the IE% and θ were improved. Also, the inhibition performance was enhanced by adding potassium iodide; so that, the inhibition order of samples was as follows: CH-3I> CH-2I> CH-I> CH

The weight loss test was performed for iron specimens in the presence of 0.3 g/L inhibitor at various temperatures for 2 h, and the data are presented in Table 2. Thermodynamic parameters were estimated for the iron dissolution using the Arrhenius equation:

$$\ln(CR) = \frac{-E_a}{RT} + lnA \quad \ldots (6)$$

and the Eyring equation:

$$ln\left(\frac{C.R.}{T}\right) = -\frac{\Delta H}{RT} + \frac{\Delta S}{R} + ln\frac{k_B}{h} \quad \ldots (7)$$

where be E_a the activation energy; R, universal gas constant; A, frequency factor; h, Plank's constant; N, Avogadro's number; ΔS, entropy and ΔH, enthalpy. By plotting the Arrhenius plot (Fig. 2A), the activation energy of inhibitor adsorption on the

Table 2 — The gravimetric results of iron in present of 0.3 g/L different inhibitors at different temperatures for 2 h.

Inhibitor	T (K)	W (g)	C.R. × 10^{-3} ($g/cm^2.h$)
CH	303	0.0584	14.60
	313	0.2077	51.93
	323	0.3003	75.07
	333	0.4477	111.93
CH-I	303	0.0570	14.25
	313	0.2138	53.45
	323	0.2620	65.50
	333	0.3265	81.62
CH-2I	303	0.0303	7.58
	313	0.1480	37.00
	323	0.2150	53.75
	333	0.3154	78.85
CH-3I	303	0.0130	32.50
	313	0.1578	39.45
	323	0.2327	58.17
	333	0.2714	67.85

Table 1 — The gravimetric results of iron in present of different inhibitors with different concentrations at 30 ˚c for 2 h.

Inhibitor	Concentration (g/L)	W (g)	θ	I.E.%	C.R. × 10^{-3} ($g/cm^2.h$)
Blank	0	0.0839	-	-	20.97
CH	0.1	0.0753	0.10	10.25	18.83
	0.3	0.0621	0.26	25.98	15.53
	0.5	0.0584	0.30	30.39	14.60
CH-I	0.1	0.0726	13.47	13.46	18.15
	0.3	0.0570	0.32	32.06	14.25
	0.5	0.0525	0.37	37.43	13.12
CH-2I	0.1	0.0462	0.49	48.51	11.55
	0.3	0.0303	0.64	63.88	7.57
	0.5	0.0248	0.70	70.44	6.20
CH-3I	0.1	0.0294	0.65	64.95	7.35
	0.3	0.0143	0.83	82.96	3.57
	0.5	0.0130	0.85	84.51	3.25

specimen surface was determined and reported in Table 3. The lower activation energy for the adsorbing an inhibitor on the metal surface indicates strong chemical adsorption; while the larger amounts of activation energy imply weak physical adsorption[17].

Table 3 shows that adding a small amount potassium iodide to chitosan, had a slight effect on the absorption mechanism of this polymer on the iron surface; so that, the activation energies for adsorption of CH, CH-I, and CH-2I had no noticeable difference and were physical. The activation energy of CH-3I adsorption had a significant decrease indicating the stronger absorption of this inhibitor than others. The comparison of IE% (Table 1) and E_a (Table 3) emphasized that The CH-3I absorption on the iron surface was stronger than the other three inhibitors. It seems that higher iodine in the chitosan structure increases the electron density of polymer and strengthens the interaction between inhibitor and metal.

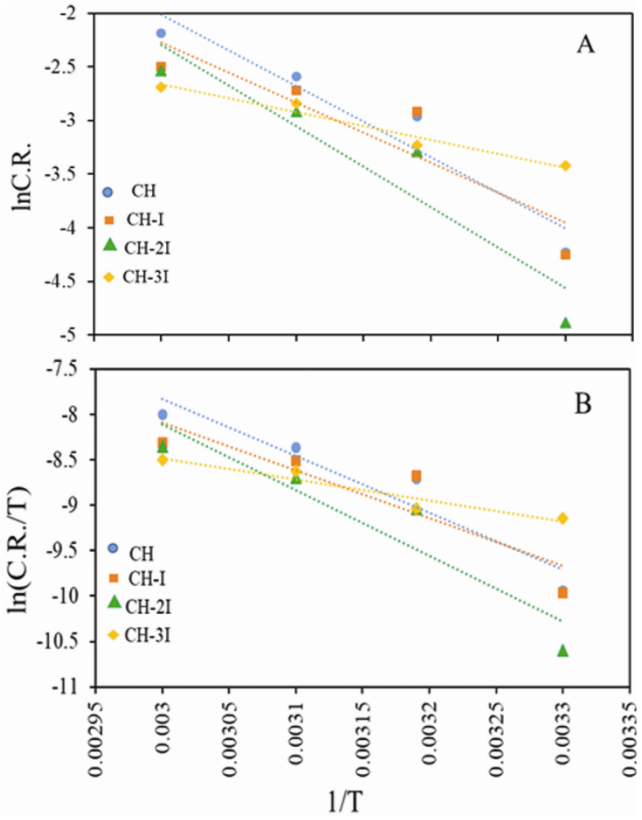

Fig. 2 — The plots of (A) Arrhenius and (B) Eyring for iron in 0.5 M H_2SO_4 solution and presence of 0.3 g/l inhibitor at different temperatures for 2 h.

Table 3 — Thermodynamics parameters of corrosion reaction for iron in 0.5 M H_2SO_4 solution in the presence of inhibitor.

Inhibitor	E_a (kJ/mol)	ΔH (kJ/mol)	ΔS (kJ/mol.K)
CH	55.03	52.29	105.73
CH-I	46.46	43.74	133.39
CH-2I	62.80	60.24	84.19
CH-3I	21.54	19.50	-209.55

Figure 2B illustrates the Eyring plot; The ΔH and ΔS were assessed from the equations of straight outlines and presented in Table 3. The positive ΔH values indicate the endothermic nature of the iron corrosion. From the negative ΔS value, it is inferred the active complex in the rate-determining step (RDS), and the metal dissolution rate are related to each other; and conversely, the positive ΔS value expresses the independency between the active complex of RDS and the metal dissolution step. Based on Table 3, the relationship between the active complex of RDS and the metal dissolution step was increased by increasing the iodine in the inhibitor structure.

The inhibitor polymer in the aqueous medium competes with H_2O molecules for the adsorption on the iron surface. In this work, the studied isotherms were[18]:

$$\text{Temkin: } \ln C = a\,\theta - \ln K \quad \ldots(8)$$

$$\text{Langmuir: } \frac{C}{\theta} = \frac{1}{k} + c \quad \ldots(9)$$

$$\text{Frumkin: } ln\frac{\theta}{C(1-\theta)} = lnK + a\theta \quad \ldots(10)$$

where be C, the concentration of the inhibitor, K_{ads}, the equilibrium adsorption constant, and θ, surface coverage. Based on gravimetric results, the plotting of three isotherms was carried out for the different inhibitors at 30°C for 2 h in 0.5 M H_2SO_4; displayed in Fig. 3. The isotherms fitting with experimental data was evaluated via comparison of the correlation coefficient (R^2); reported in Table 4. The results demonstrated that the adsorption of the inhibitors on the iron surface obeyed the Langmuir. It is deduced from the results that the adsorbed molecules are located on active sites onto the iron

Table 4 — The correlation coefficients for the adsorption isotherms of inhibitors on iron surface.

Isotherm	CH	CH-I	CH-2I	CH-3I
Langmuir	0.826	0.986	1.000	0.995
Temkin	0.719	0.918	0.993	0.847
Frumkin	0.011	0.148	0.958	0.182

surface as a monolayer; without any interactions between them. Concerning the selected isotherms and its function, the constant of adsorption equilibrium (K) was obtained for the adsorption of four inhibitors; then, the eq. 11 was utilized to compute the standard free energy (ΔG); listed in Table 5.

$$\Delta G = -RTln(55.5K) \quad \ldots(11)$$

R and T are defined above. The 55.5 signifies the molar H_2O concentration in the corrosive medium.

Table 5 — Effect of Inhibitors on equilibrium constant and standard free energy of iron corrosion based on Langmuir isotherm.

Inhibitor	CH	CH-I	CH-2I	CH-3I
K ($mol^{-1}.lit^{-1}$)	1.558	1.5463	1.104	1.039
ΔG (J/mol)	-11235.37	-11215.84	-10367.08	-10214.21

The negative ΔG value proves the absorption of inhibitors on the iron surface was a spontaneous phenomenon. It is known that $\Delta G \leq -20$ $kJmol^{-1}$ is indicative of physical adsorption via electrostatic interactions; whereas, $\Delta G \geq -40$ $kJmol^{-1}$ is indicant of chemical adsorption via the sharing or transfer of electrons[19]. The results of the present work show the physical absorption of proposed inhibitors on the iron surface.

Scanning electron microscope analysis

Figure 4 shows scanning electron microscopy micrographs of the iron surface corroded in the acidic media without and with the inhibitor. Figure 4A shows a rough surface after iron corrosion, which indicates the dissolution of corrosion products. Comparison of Fig. 4A with Fig. 3B-3E revealed the

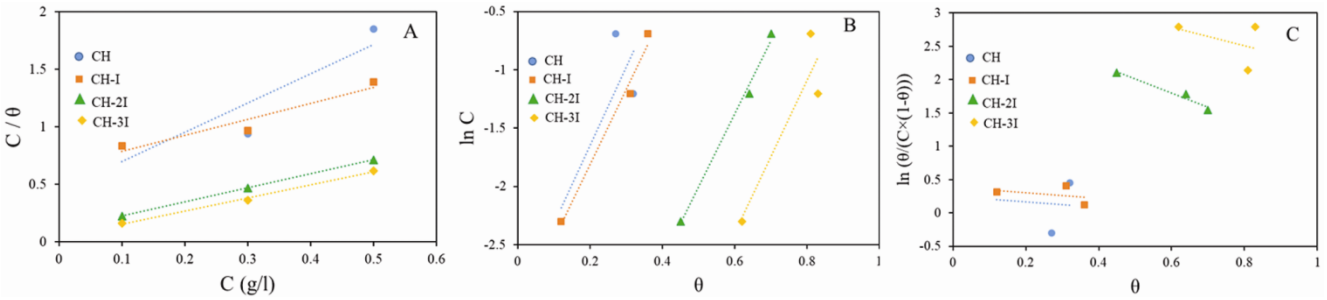

Fig. 3 — The plots of (A) Langmuir, (B) Temkin and (C) Frumkin isotherms for the different inhibitors at 30 ˚c for 2 h based on gravimetric results in 0.5 M H_2SO_4 solution.

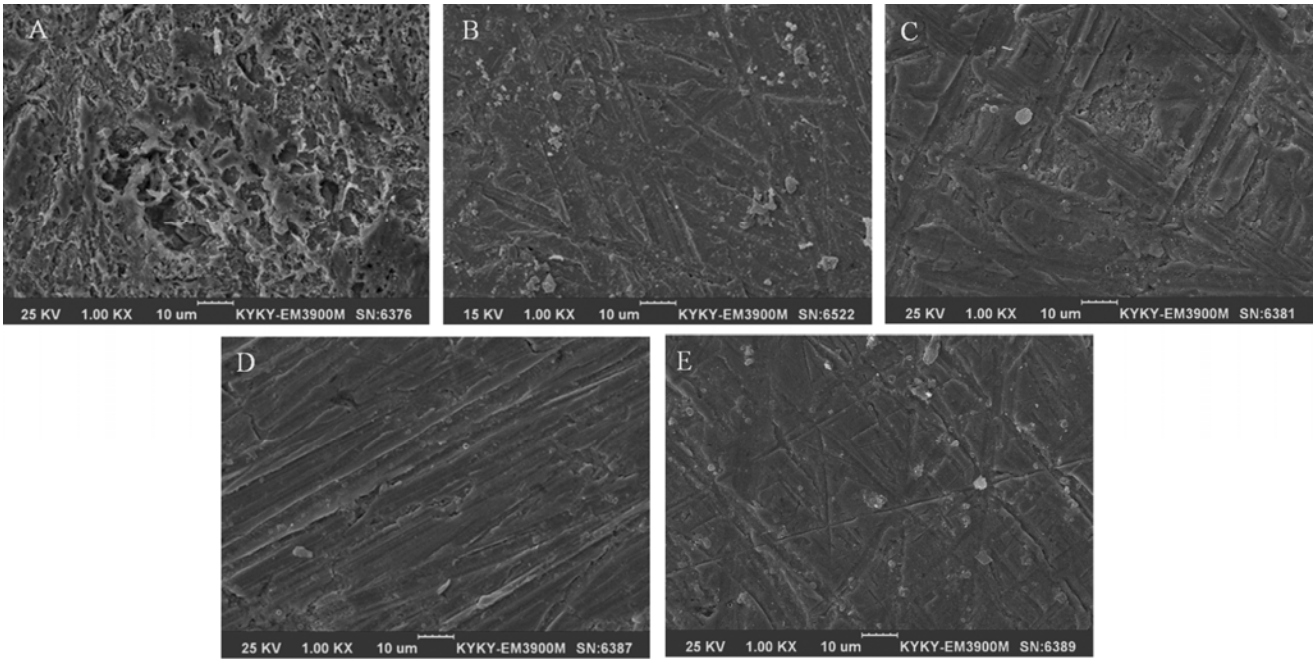

Fig. 4 — SEM micrographs of iron surface after immersion in 0.5 M H_2SO_4 solution, (A) in absence of inhibitor (Blank), in the presence of 5 g/l (B) CH, (C) CH-I, (D) CH-2I and (E) CH-3I inhibitor.

inhibitory strength of the proposed components in the present work. It is observed the iodine increasing to chitosan structure had caused the iron surface to be flat in Fig. 3C-3E; which indicated a decrease in iron corrosion

Electrochemical Impedance spectroscopy

The curves of Nyquist, bod *Z*, and phase, are presented for the iron specimens in the absence and 0.5 g /L of inhibitor and 0.5 M sulfuric acid as the corrosive solution at OCP and frequency of 0.1 Hz to 10 kHz in Fig. 5; the impedance parameters are reported for the equivalent electrical circuit as $[R_s(C_f[R_f(QR_{ct})])]$ in Table 6. In the proposed circuit, R_s represents the electrical resistance of corrosive medium; which according to Table 6, it was less than 3.5 Ω; because sulfuric acid, as a strong acid, is easily ionized in water and ions can decrease the solution resistance. Respectively, C_f and R_f indicate the capacitance and capacitive resistance. By adding inhibitor to the solution, the adsorption of the inhibitor happens at the specimen surface (solid / liquid phase interface). This phenomenon causes a variation in the potential difference between the iron and the electrolyte, due to the non-uniformity in the distribution of electrical charges in the interface. The double electric layer is effective in the properties of the interface[20].

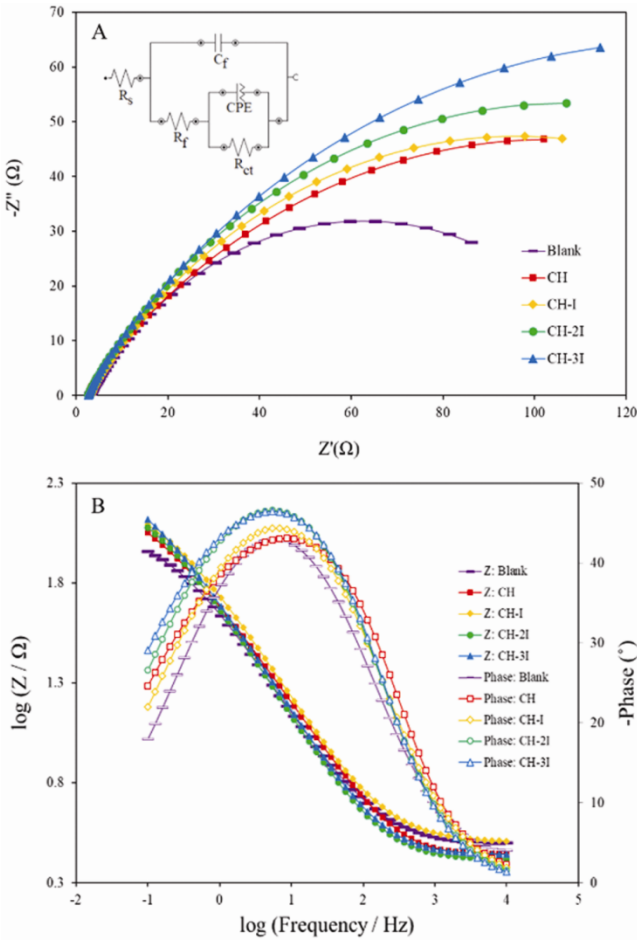

Fig. 5 — The plots of (A) Nyquist (Inset: equivalent electrical circuit) and (B) Bode for iron corrosion in 0.5 M H_2SO_4 solution at OCP and 0.1 Hz to 10 kHz.

The inhibitor entry into the electrical double layer causes to be changed the layer structure and composition. Therefore, the measuring dual-layer capacity before and after the addition of inhibitor can be used to determine the adsorption rate. According to Table 6, the inhibitor addition increased the C_f; so the adsorption of the inhibitors was confirmed on the iron surface. If a capacitance behavior can't be satisfactorily shown by the capacitor, instead of the capacitor, a constant phase element (CPE) is used and represented by *Q*. Based on the fitted circuit with experimental results, a slight dual layer is formed as CPE with main capacitive layer in some places on the metal surface. The admittance function of this element is defined as:

$$Y_Q = Y_0(j\omega)^n \quad \ldots(12)$$

where Y_0 is the capacity, *n*, the roughness degree of the surface (between -1 and +1), j, the imaginary root, and ω, the angular frequency.

Table 6 — Impedance parameters for corrosion iron in 0.5 M H_2SO_4 with 0.5 g/l inhibitor based on $[R_s(C_f[R_f(QR_{ct})])]$ at OCP and 0.1 Hz to 10 kHz.

Inhibitor	OCP (V)	R_s (Ω)	C_f (μF)	CPE		R_{ct} (Ω)	χ	I.E.%
				Y_0 (mMho)	n			
Blank	-0.597	3.35	24.7	5.80	0.62	120	0.052	-
CH	-0.667	3.21	131	5.16	0.59	188	0.079	36.17
CH-I	-0.668	2.81	115	6.48	0.54	204	0.046	41.18
CH-2I	-0.684	2.61	209	6.23	0.59	211	0.027	43.13
CH-3I	-0.682	2.76	222	6.23	0.57	265	0.031	54.72

The resistance of charge transfer (R_{CT}) is presented in Table 6 for the corrosion of iron without and with of various inhibitors. As it is known, the addition of the inhibitor has increased the R_{CT}. The IE% was obtained using the inverse of charge transfer resistance ($R^{-1}{}_{ct}$) through [11]:

$$IE\% = \frac{R_{ct\,Blank}^{-1} - R_{ct}^{-1}}{R_{ct\,Blank}^{-1}} \times 100 \quad \ldots(13)$$

The IE% comparison for different inhibitors under the same conditions is under the obtained sequence in the gravimetric section. This indicates the improved adsorption on the iron surface and the synergistic influence of iodine ion and chitosan on the inhibition performance.

Potentiodynamic polarization

The polarization Tafel curves are illustrated for iron in the different inhibitors concentrations and 0.5 M H_2SO_4 solution in Fig. 6; Table 7 lists the gotten results for four inhibitors. The shifting corrosion potential (E_{cor}) in the negative and positive directions, is respectively because of slow down the cathode and anode half-reactions[21]. The corrosion reaction involves the creation of intermediate species of corrosive agent adsorption with metal surface atoms like FeOH. The production of intermediate species is affected by the inhibitors. Hence, the inhibitor presence would change the Tafel slopes for anodic and cathodic branches. Based on Table 7 and the E_{cor} comparison, the potential change is seen positively and negatively, together. On the other hand, the simultaneous evolution of the andic and cathodic slopes with the addition of inhibitor confirmed the inhibitory effect on the anode and cathode half-reactions. It is concluded that the proposed compounds have been of mixed inhibitor type.

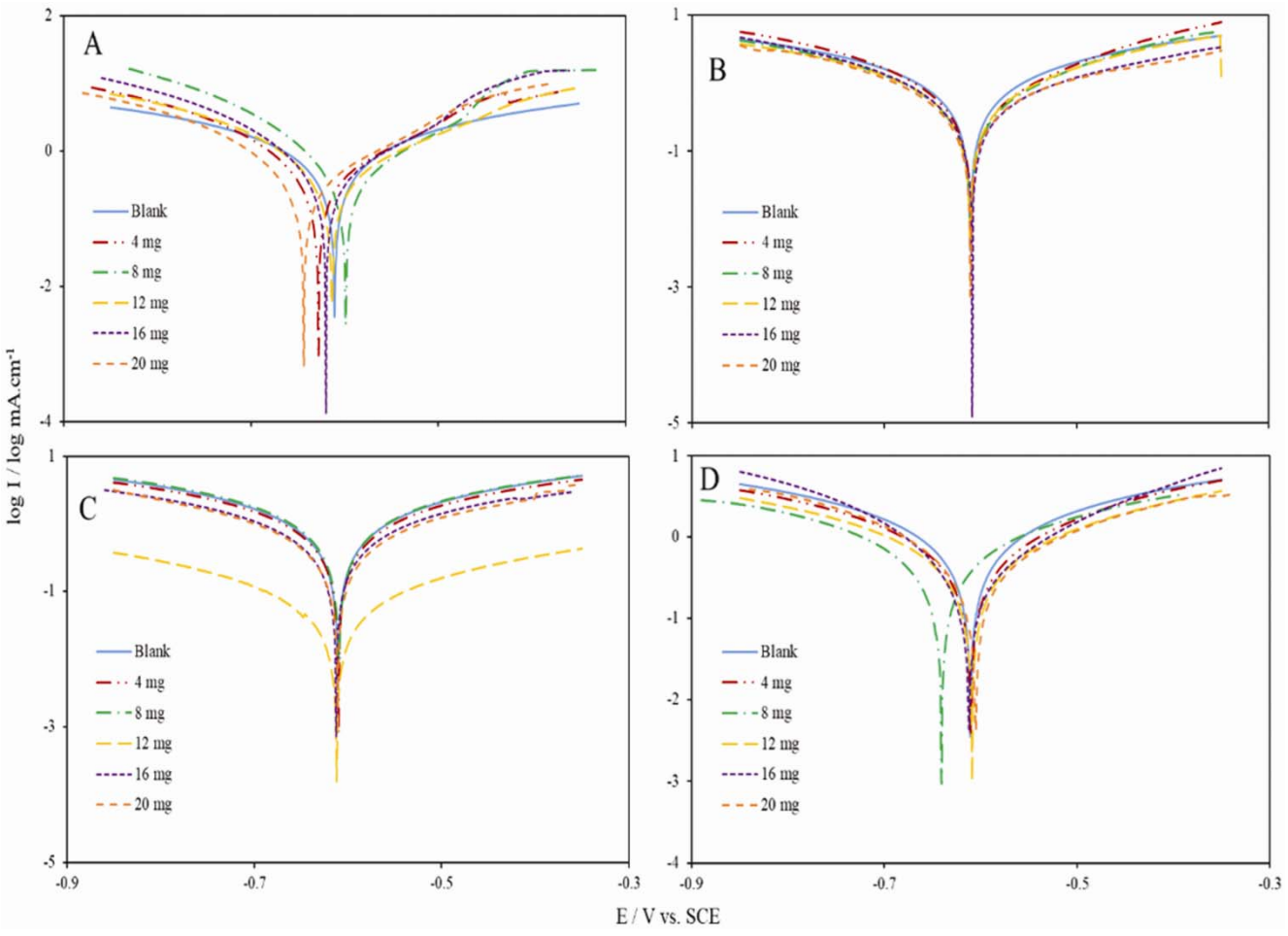

Fig. 6 — The polarization Tafel curves for iron in the different concentrations of (A) CH, (B) CH-I, (C) CH-2I and (D) CH-3I and 0.5 M H_2SO_4 with 50 mV/s scan rate.

Table 7 — Polarization parameters and efficiency of corrosion inhibition on iron surface by inhibitors in 0.5 M H_2SO_4 at 25 °C.

Inhibitor	Concentration mg/l	OCP (V)	E_{cor} (v)	β_a (V/dec)	β_c (V/dec)	R_p (Ω)	I_{cor} (mA/cm^2)	Corrosion rate (mpy)	%I.E.	θ
Blank	0	-0.600	-0.611	0.11	0.09	55.28	0.389	177.67	-	-
CH	4	-0.616	-0.628	0.10	0.14	66.09	0.373	170.37	4.11	0.04
	8	-0.585	-0.599	0.08	0.12	57.49	0.367	167.76	5.66	0.06
	12	-0.600	-0.614	0.10	0.13	68.41	0.360	164.71	7.46	0.07
	16	-0.608	-0.620	0.08	0.10	60.15	0.323	147.55	16.97	0.17
	20	-0.639	-0.644	0.10	0.12	76.09	0.311	142.21	20.05	0.20
CH-I	4	-0.602	-0.610	0.11	0.12	66.92	0.358	163.798	7.97	0.08
	8	-0.601	-0.611	0.12	0.13	77.33	0.351	160.23	9.77	0.10
	12	-0.601	-0.610	0.10	0.11	74.36	0.311	141.98	20.05	0.20
	16	-0.600	-0.609	0.11	0.12	82.90	0.299	136.87	23.14	0.23
	20	-0.601	-0.611	0.11	0.12	87.89	0.293	133.996	24.68	0.25
CH-2I	4	-0.603	-0.610	0.10	0.10	61.51	0.350	159.50	10.02	0.10
	8	-0.602	-0.609	0.09	0.08	52.46	0.348	158.91	10.54	0.11
	12	-0.606	-0.612	0.12	0.11	75.28	0.328	150.01	15.68	0.16
	16	-0.604	-0.613	0.13	0.12	82.91	0.322	147.23	17.22	0.17
	20	-0.605	-0.611	0.11	0.11	93.75	0.252	115.33	35.22	0.35
CH-3I	4	-0.601	-0.610	0.10	0.11	74.36	0.311	141.98	20.05	0.20
	8	-0.633	-0.641	0.12	0.12	85.22	0.295	134.81	24.16	0.24
	12	-0.598	-0.609	0.12	0.11	93.62	0.272	124.22	30.08	0.30
	16	-0.604	-0.612	0.10	0.12	92.39	0.248	113.45	36.25	0.36
	20	-0.595	-0.605	0.08	0.09	89.12	0.207	94.56	46.79	0.47

Conclusion

Four samples of chitosan-iodide with different ratios were prepared as the inhibitor of iron corrosion in the acidic medium, and the synergic influence of chitosan and iodide was studied in this research. The inhibition performance enhanced with increasing chitosan concentration. It was significantly improved in the presence of potassium iodide. The results showed that the introduced inhibitors were of the interface inhibitors → liquid phase → mixed type with the physical adsorption. The adsorption of iodized chitosan on the iron surface is compiled Langmuir isotherm. These inhibitors, by changing the electrical double layer, increased the resistance of charge transfer. The experimental data demonstrated that the doping iodide ion to chitosan structure was capable on the surface coverage of the inhibitor. It appeared that the incorporation of iodide in the polymer structure improved the electron density of polymer and strengthened the interaction between inhibitor and metal.

References

1 Eddy N O, Odoemelamc S A & Ekwumemgbo P, *Sci Res Essays,* 4 (2009) 33.
2 Sastri V S, *John Wiley*, New York, (1998) 39.
3 Roberge P R, *McGraw-Hill*, New York. (2000).
4 Kabanda M M, Murulana L C & Ebenso E E, *Int J Electrochem Sci,* 7 (2012) 7179.
5 Nazeer A A, El-Abbasy H M & Fouda A S, *Res Chem Intermediat*, 39 (2013) 921.
6 Ebenso E E, Arslan T & Kandemirli F, *Int J Quantum Chem*, 110 (2010) 2614.
7 Shaban S M, Aiad I, Moustafa A H & Aljoboury O H, *J Mol Liq*, 273 (2019) 164.
8 Tiu B D B & Advincula R C, *React Funct Polym*, 95 (2015) 25.
9 Nilsen-Nygaard J, Strand S P, Vårum K M, Draget Kurt I & Nordgård Catherine T, *Polymers,* 7 (2015) 552.
10 Ekrami-Kakhki M S, Khorasani-Motlagh M & Noroozifar M, *J Appl Electrochem,* 41 (2011) 527.
11 Larabi L, Harek Y, Traisnel M & Mansri A, *J Appl Electrochem*, 34 (2004) 833.
12 Chetouani A, Medjahed K, Benabadji K E, Hammouti B, Kertit S & Mansri A, *Prog Org Coat*, 46 (2003) 312.
13 Herbert R W R & Uhlig H, *John Wiley & Sons*, New Jersey, (2008).
14 Abd El Aal E E, Abd El Wanees S, Farouk A & Abd El Haleem S M, *Corros Sci,* 68 (2013) 14.
15 Gopiraman M, SakunthalaP, Kesavan D, Alexramani V, Kim I S & Sulochana N, *J Coat Technol Res,* 9 (2012) 15-26.
16 AyyannanG, Karthikeyan K, Vivekananthan S, Gopiraman M & Rathinavelu A, *Ionics,* 19 (2013) 919.
17 Dehdab M, Yavari Z, Darijani M & Bargahi A, *Desalination,* 400 (2016) 7.
18 TianH, Cheng Y F, Li W & Hou W, *Corros Sci*, 100 (2015) 341.
19 Wang D, Xiang B, Liang Y, Song S & Liu C, *Corros Sci*, 85 (2014) 77.
20 McCafferty E, *Springer-Verlag*, New York, (2010).
21 Rosliza R, Senin H B & Wan Nik W B, *Aspects*, 312 (2008) 185.